AIP Advances

Corrugated flat band as an origin of large thermopower in hole doped $PtSb_2$

Cite as: AIP Advances **2**, 042108 (2012); https://doi.org/10.1063/1.4759007
Submitted: 26 July 2012 . Accepted: 24 September 2012 . Published Online: 08 October 2012

Kouta Mori, Hidetomo Usui, Hirofumi Sakakibara, and Kazuhiko Kuroki

Corrugated flat band as an origin of large thermopower in hole doped $PtSb_2$

Kouta Mori,[1,3] Hidetomo Usui,[1,3] Hirofumi Sakakibara,[2]
and Kazuhiko Kuroki[1,3]
[1]*Department of Engineering Science, The University of Electro-Communications, Chofu, Tokyo 182-8585, Japan*
[2]*Department of Applied Physics and Chemistry, The University of Electro-Communications, Chofu, Tokyo 182-8585, Japan*
[3]*JST, ALCA, Sanbancho, Chiyoda, Tokyo 102-0075, Japan*

(Received 26 July 2012; accepted 24 September 2012; published online 8 October 2012)

The origin of the recently discovered large thermopower in hole-doped $PtSb_2$ is theoretically analyzed based on a model constructed from first principles band calculation. It is found that the valence band dispersion has an overall flatness combined with some local ups and downs, which gives small Fermi surfaces scattered over the entire Brillouin zone. The Seebeck coefficient is calculated using this model, which gives good agreement with the experiment. We conclude that the good thermoelectric property originates from this "corrugated flat band", where the coexistence of large Seebeck coefficient and large electric conductivity is generally expected. [http://dx.doi.org/10.1063/1.4759007]

Good thermoelectric materials are those materials that can transform heat into electricity with high efficiency. The efficiency of thermoelectric materials is characterized by the dimensionless figure of merit, ZT, where T is the temperature, and $Z = S^2\sigma/\kappa$ with S, σ and κ being the Seebeck coefficient, electric conductivity, and the thermal conductivity, respectively.[1] In particular, the product $P = S^2\sigma$ is called the power factor, and a material with large P requires a large S and σ. It is known, however, that materials with large Seebeck coefficient usually have small conductivity, so that good thermoelectric materials are often found in semiconducting materials with rather small amount of carriers.

In this context, the discovery of good thermoelectric properties in the sodium cobaltate Na_xCoO_2[2] has been of special interest in that a large power factor is observed in a material with large amount of doped holes and thus metallic conductivity. There have been various theoretical studies on this material,[3–6] and in particular, one of the present authors along with Arita proposed that a peculiar band shape named the "pudding mold type" (Fig. 1(b)) is the origin of this coexistence of good conductivity and large thermopower.[6] Namely in a system having a band with flat portion at the top (or bottom), connecting into a dispersive portion, the Fermi level is kept close to the band edge upon doping, and this gives rise to a large group velocity difference between electrons and holes, resulting in a large Seebeck coefficient. At the same time, the large group velocity of holes due to the dispersive portion of the band gives a large electric conductivity, and this combination results in a large power factor.

Quite recently, Nishikubo *et al.* discovered that doping holes into a cubic pyrite material $PtSb_2$ by partially substituting Pt by Ir as $Pt_{1-x}Ir_xSb_2$ gives rise to a coexistence of metallic conductivity and a large Seebeck coefficient.[7] Refering to the band structure calculation in ref. 8, a possible relevance of the peculiar band structure has been pointed out. In the present paper, we present first principles band calculation result of $PtSb_2$, and analyze the origin of the good thermoelectric properties of this material. It is shown that the material has a valence band dispersion with an overall flatness but with some local ups and downs. This band structure, which we refer to as the "corrugated flat band"

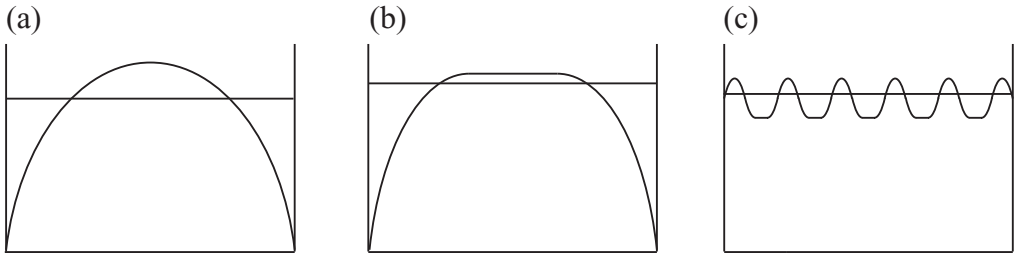

FIG. 1. A schematic image of (a) usual metal band (b) pudding mold band (c) corrugated flat band. The horizontal lines are image of the position of the Fermi level that gives the same Fermi surface volume.

(Fig. 1(c)), has some similarity with the pudding mold band in that they both have coexisting flatness and the large group velocity, but still is different from the pudding mold band in that the flatness extends over the entire Brillouin zone, while the dispersiveness (the corrugation) is a local feature which appears at various points all over the Brillouin zone.

First principles band calculation of $PtSb_2$ is performed using the Wien2K package.[9] We use the experimentally determined lattice structure given in ref. 10 The spin-orbit coupling, which turns out to have only small effect, is omitted in the present results. The calculation result is shown in Fig. 2(a) (dashed lines). The bands near the Fermi level mainly consists of Sb 5*p* orbitals, mixed with Pt 5*d* orbitals. The upper most valence band originates almost solely from Sb 5*p* orbitals, and the near absence of the *d* orbital character, namely, the non-bonding nature (non-bonding in the sense that *p* does not mix with *d*), makes this band relatively flat compared to other bands with 5*p* character. On the other hand, this upper most valence band is not perfectly flat, and there are some ups and downs, which we will call "corrugations". This corrugation give rise to small pocket like Fermi surfaces when holes are doped as we shall see below.

From this band calculation, we obtain maximally localized Wannier orbitals[11,12] mainly consisting of Sb 5*p* orbitals, which enables us to construct a 24 orbital (eight Sb per unit cell × three 5*p* orbitals) tightbinding model that correctly reproduces the original first principles band structure around the Fermi level (Fig. 2(a), solid lines). We consider doping holes into this model assuming a rigid band, where the doping ratio δ is defined as $\delta = (24 - n)/4$ with n being the total band filling. In an ideal situation, this δ corresponds to the experimental substitution ratio x. In Fig. 3, we show the Fermi surface for three doping ratios. The combination of the overall flatness and the corrugation of the valence band results in multiple Fermi surface pockets that are scattered over the entire Brillouin zone.

Based on this model, we calculate the Seebeck coefficient using the Boltzmann's equation approach.

$$\mathbf{S} = \frac{1}{eT}\mathbf{K}_0^{-1}\mathbf{K}_1 \tag{1}$$

where $e(<0)$ is the electron charge, T is the temperature, tensors $\mathbf{K}_0$ and $\mathbf{K}_1$ are given by

$$\mathbf{K}_n = \sum_{\boldsymbol{k}} \tau \boldsymbol{v}(\boldsymbol{k})\boldsymbol{v}(\boldsymbol{k}) \left[-\frac{\partial f(\varepsilon)}{\partial \varepsilon}(\boldsymbol{k}) \right] (\varepsilon(\boldsymbol{k}) - \mu)^n. \tag{2}$$

Here, $\varepsilon(k)$ is the band dispersion of the tight binding model, $\boldsymbol{v}(\boldsymbol{k}) = \nabla_{\boldsymbol{k}}\varepsilon(\boldsymbol{k})$ is the group velocity, τ is the quasiparticle lifetime, which will be taken as a constant in the present study. $f(\varepsilon)$ is the Fermi distribution function, and μ is the chemical potential determined from the band filling. Hereafter, we simply refer to $(\mathbf{K}_n)_{xx}$ as K_n, and $S_{xx} = (1/eT)(K_1/K_0)$ (for diagonal $\mathbf{K}_0$) as S. Using K_0, conductivity can be given as $\sigma_{xx} = e^2K_0 \equiv \sigma = 1/\rho$.

In Fig. 4(a), we show the doping ratio dependence of the Seebeck coefficient at $T = 300$ K. It can be seen that the calculation results are in overall agreement with the experiment.[13] In Fig. 4(b), we show the temperature dependence of the Seebeck coefficient. This is also in fair agreement with the experiment, although the steep increase at very low temperatures seen experimentally is not found in the calculation. In particular, the broad maximum at around $T = 400$ K observed for

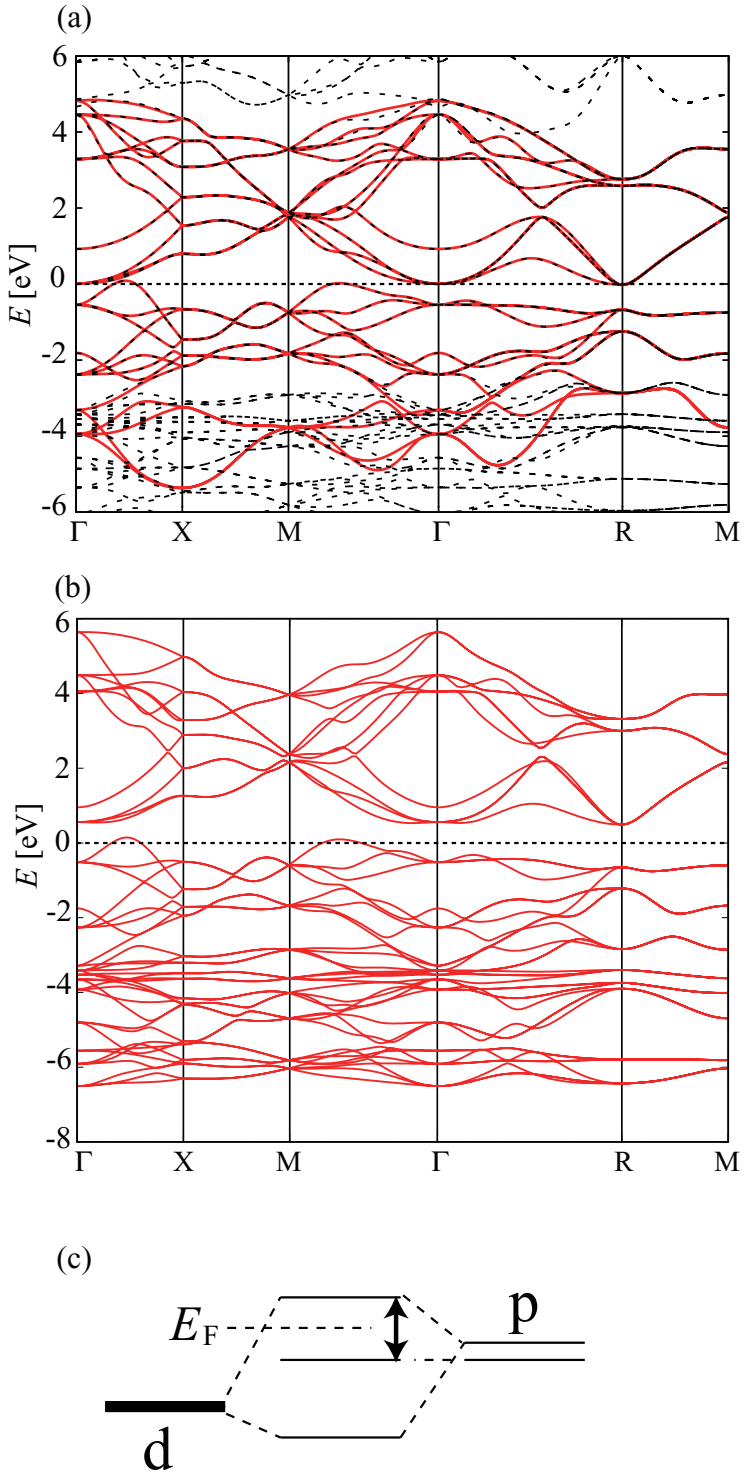

FIG. 2. (a) Dashed lines : the first principles band calculation result of $PtSb_2$. Red solid lines : the band structure of the 24 orbital model. (b) The band structure of 44 orbital *p-d* model with all of the *d-p* hybridization multiplied by a factor of 1.2. (c) A schematic figure of the *p-d* hybridization and the band gap.

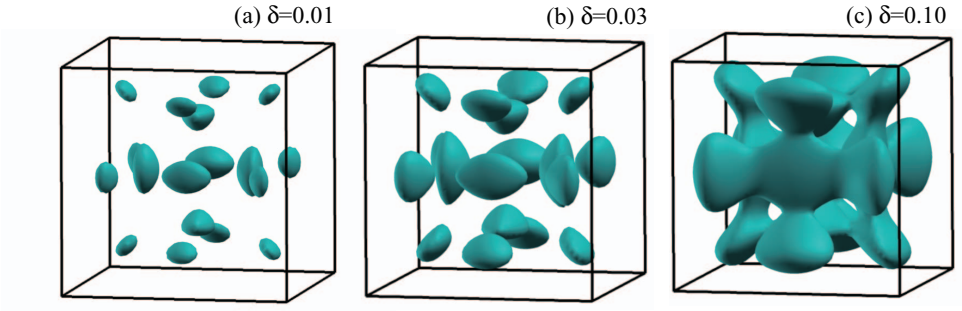

FIG. 3. The Fermi surface of the 24 band model for (a) $\delta = 0.01$ (b) 0.03 (c) 0.1.

$x = 0.01$ is roughly reproduced theoretically. This maximum is due to the presence of the conduction band lying close to the Fermi level, which gives a negative contribution to the Seebeck coefficient at high temperatures. We will come back to this point later.

In Fig. 4(c), we show the normalized power factor as a function of the doping. It can clearly be seen that a large power factor arises in the hole doped regime, where the Fermi level lies in the corrugated flat band. This good thermoelectric property can be understood as follows. In metallic systems, where the Fermi level lies within the energy bands, it is generally required to keep the Fermi level close to the band edge in order to obtain a large Seebeck coefficient. This is because the Seebeck effect is caused by the difference of the group velocity between electrons and holes in the vicinity of the Fermi level, and the two velocities differ largely (the ratio of the group velocities above and below the Fermi level is large) near the band edge. However, keeping the Fermi level close to the band edge usually means that the number of doped carriers is small, so that the absolute values of the group velocity and the volume of the Fermi surface is both small, resulting in a small electric conductivity. Similar to the case of the pudding mold band,[6] the situation is largely different in the case of the corrugated flat band. As mentioned above, multiple Fermi pockets are scattered over the entire Brillouin zone due to the flatness of the conduction band. This situation is schematically shown in Fig. 1(c) along with the case of a usual metal with a single Fermi surface Fig. 1(a). The overall flatness of the bands and thus the large multiplicity of the Fermi surface prevents the Fermi level from quickly lowering upon hole doping, giving rise to a large Seebeck coefficient even for large amount of hole doping. At the same time, the existence of multiple Fermi surfaces together with a large group velocity due to the corrugation results in a large electric conductivity. The combination of these effects results in a large power factor. In other words, in a corrugated flat band, the multi-valley effect seen in some of the thermoelectric semiconducting materials[1] is enhanced in an ultimate way in that the overall flatness of the band extends over the entire Brillouin zone.

As seen from the above, the corrugated flat band is indeed a favorable band structure for large thermopower, but there exists a flaw in the present material in that the conduction band lies too close to the valence band. The conduction band gives a negative contribution, so that the Seebeck coefficient decreases at high temperatures. Since the band gap opens between the nonbonding and the antibonding *p*-*d* bands as shown in Fig. 2(c), a larger band gap is expected to open for larger *p*-*d* hybridization, where the bonding-antibonding splitting becomes large. To see this effect, we construct a 44 orbital model which explicitly considers 20 (5 orbitals $\times$ 4 sites) Pt 5*d* and 24 Sb 5*p* orbitals, and increase all of the hopping integrals between *p* and *d* orbitals by a factor of 1.2 hypothetically by hand. The obtained band structure is shown in Fig. 2(b). For such a band structure, the Seebeck coefficient continues to increase for high temperatures as shown in Fig. 3(b) (dashed line).

To summarize, we have shown that the recently found good thermoelectric properties of $PtSb_2$ is due to the presence of the corrugated flat band, which gives rise to multiple Fermi pockets scattered over the entire Brillouin zone. The flatness of the band originates from the non-bonding character of the Sb *p* band, while the corrugation of this band mainly comes from the direct *p*-*p* hoppings. The multiplicity of the Fermi surface results in a coexistence of large Seebeck coefficient and a good

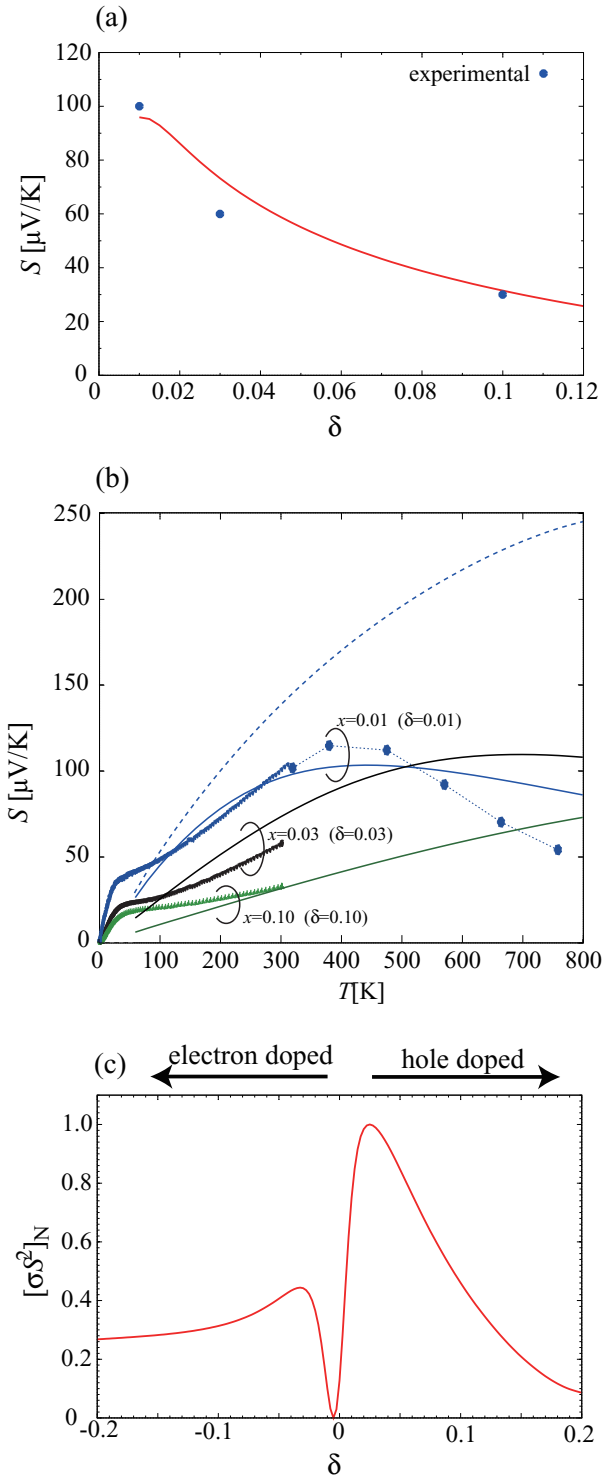

FIG. 4. (a) The calculated Seebeck coefficient against the doping ratio δ at $T = 300$ K. The dots are the experimental data from ref. 7 (b) The Seebeck coefficient against the temperature for various doping ratios. (Connected) symbols are the experimental data from ref. 7. Upper most dashed line is the result for the hypothetical band structure shown in Fig. 2(b) with $\delta = 0.01$. (c) The power factor (normalized with its maximum value) against the doping ratio for $T = 300$ K.

metallic conductivity, giving rise to a large power factor. The present mechanism for large power factor is rather general, and is expected to take place where bands with non-bonding character is present near the Fermi level. Despite the presence of the corrugated flat band, one flaw of $PtSb_2$ is the narrowness of the band gap. The conduction band lying close to the valence band gives a negative conductivity to the Seebeck coefficient at high temperatures. We expect that materials with the combination of a corrugated flat band along with a wider band gap should result in even more ideal thermoelectric properties.

ACKNOWLEDGMENTS

We are grateful to M. Nohara for showing us the experimental results prior to publication. H.S. acknowledges support from JSPS.

[1] For a general review on the theoretical aspects as well as experimental observations of thermopower, see, G. D. Mahan, Good Thermoelectrics, Solid State Physics **51**, 81 (1997).
[2] I. Terasaki, Y. Sasago, and K. Uchinokura, Phys. Rev. B **56**, R12685 (1997).
[3] D. J. Singh, Phys. Rev. B **61**, 13397 (2000).
[4] W. Koshibae, K. Tsutsui, and S. Maekawa, Phys. Rev. B **62**, 6869 (2000).
[5] W. Koshibae and S. Maekawa, Phys. Rev. Lett. **87**, 236603 (2001).
[6] K. Kuroki and R. Arita, J. Phys. Soc. Jpn. **76**, 083707 (2007).
[7] Y. Nishikubo, S. Nakano, K. Kudo, and M. Nohara, Appl. Phys. Lett. **100**, 252104 (2012).
[8] P. R. Emtage, Phys. Rev. B **138**, A246 (1965).
[9] P. Blaha, K. Schwarz, G. K. H. Madsen, D. Kvasnicka, and J. Luitz, *Wien2k: An Augmented Plane Wave + Local Orbitals Program for Calculating Crystal Properties* (Vienna University of Technology, Wien, 2001). Here we take $RK_{\max} = 10$, 1024 k-points, and adopt the exchange correlation functional introduced by J. P. Perdew, K. Burke, and M. Ernzerhof, [Phys. Rev. Lett. **77**, 3865 (1996)].
[10] N. E. Brese and H. G. Von Schnering, Z. Anorg. Allg. Chem. **620**, 393 (1994).
[11] N. Marzari and D. Vanderbilt, Phys. Rev. B **56**, 12847 (1997); I. Souza, N. Marzari, and D. Vanderbilt, Phys. Rev. B **65**, 035109 (2001). The Wannier functions are generated by the code developed by A. A. Mostofi, J. R. Yates, N. Marzari, I. Souza, and D. Vanderbilt, (http://www.wannier.org/).
[12] J. Kunes, R. Arita, P. Wissgott, A. Toschi, H. Ikeda, and K. Held, Comp. Phys. Commun. **181**, 1888 (2010).
[13] Here we omit the calculation result for the non-doped case. This is because the Seebeck coefficient for $\delta = 0$ is very sensitive to the band gap, which cannot be estimated with enough accuracy in DFT calculations, especially when the gap is small.